An Automated Machine Vision Based System for Fruit Sorting and Grading

Chandra Sekhar Nandi
University Institute of Technology.
The University of Burdwan
Burdwan, India
chandrasekharnandi@gmail.com

Bipan Tudu
IEE Department
Jadavpur University
Kolkata, India
bip_123@rediffmail.com

Chiranjib Koley
Electrical Engineering Department
National Institute of Engineering
Durgapur, India
chiranjib@ieee.org

Abstract—**The paper presents a computer vision based system for automatic grading and sorting of agricultural products like Mango (Mangifera indica L.) based on maturity level. The application of machine vision based system, aimed to replace manual based technique for grading and sorting of fruit. The manual inspection poses problems in maintaining consistency in grading and uniformity in sorting. To speed up the process as well as maintain the consistency, uniformity and accuracy, a prototype computer vision based automatic mango grading and sorting system was developed. The automated system collect video image from the CCD camera placed on the top of a conveyer belt carrying mangoes, then it process the images in order to collects several relevant features which are sensitive to the maturity level of the mango. Finally the parameters of the individual classes are estimated using Gaussian Mixture Model for automatic grading and sorting.**

Keywords—machine vision; fruit grading and sorting; video image; maturity prediction; Gaussian mixture model

I. INTRODUCTION

Automated grading and sorting of agricultural products are getting special interest because of increased demand in different quality food with relative affordable prices by the different group of customers belongs to different living standards. Thus fruit produced in the garden are sorted according to quality and maturity level and then transported to different standard markets at different distances based on the quality and maturity level. Sorting of fruits according to maturity level is most important in deciding the market it can be sent on the basis of transportation delay.

In present common scenario, sorting and grading of fruit according to maturity level are performed manually before transportation. This manual sorting by visual inspection is labour intensive, time consuming and suffers from the problem of inconsistency and inaccuracy in judgement by different human. Which creates a demand for low cost exponential reduction in the price of camera and computational facility adds an opportunity to apply machine vision based system to assess this problem.

The manual sorting of fruits replaced by machine vision with the advantages of high accuracy, precision and processing speed and more over non-contact detection is an inevitable trend of the development of automatic sorting and grading systems [1]. The exploration and development of some fundamental theories and methods of machine vision for pear quality detection and sorting operations has been accelerate the application of new techniques to the estimation of agricultural products' quality [2].

Many color vision systems have been developed for agricultural grading applications. These applications include direct color mapping system to evaluate the quality of tomatoes and dates [3], automated inspection of golden delicious apples using color computer vision [4].

In recent years, machine vision based systems has been used in many applications requiring visual inspection. As examples, a color vision system for peach grading [5], computer vision based date fruit grading system [6], machine vision for color inspection of potatoes and apples [7], and sorting of bell peppers using machine vision [8]. Some machine vision systems are also designed specifically for factory automation tasks such as intelligent system for packing 2-D irregular shapes [9], versatile online visual inspections [10], [11], automated planning and optimization of lumber production using machine vision and computer tomography [12], camera image contrast enhancement for surveillance and inspection tasks [13], patterned texture material inspection [14], and vision based closed-loop online process control in manufacturing applications [15].

With this back ground, the proposed technique applies machine vision based system to predict the maturity level of mango from its RGB image frame, collected with the help of a CCD camera. The materials and method are discussed in Section II. Details preprocessing of image is discussed in Section III. Different feature extraction methods are discussed in Section IV. The theory of GMM is discussed in Section V, and the result and discussion in Section VI. We summarize our work and conclude this paper in Section VII.

II. MATERIALS AND METHOD

A. Sample Collection

For the experimental works total 600 number of unsorted mangoes of four varieties locally termed as "Kumrapali" (KU),"Sori" (SO),"Langra" (LA) and "Himsagar" (HI) were collected from three gardens, located at different places of West Bengal, India. Collection of mangoes were performed in three batches with an interval of one week in between batches and in each batch 200 numbers of mango were collected, having 50 numbers of each variety i.e. KU, SO, LA and HI. Steps were taken to ensure randomness in mango collection process from the gardens in each batch. After collection of mangoes each mango were tagged with some unique number generated on the basis of variety, name of the origin garden, batch number and serial number etc. Three independent human experts work in the relevant field were selected for manual prediction of maturity.

Each mango was used to pass through a conveyer belt every day until it rotten and was presented to the experts (after removing tags) for recording of human expert predicted maturity level. Then the mangoes were stored in a manner as used during transportation.

B. Experimental Procedure

A schematic diagram of the proposed automated system is shown in Fig.1, the camera used in the study was a 10 megapixel CCD camera (Olympus E-520) with maximum frame rate of 30 frames/sec.

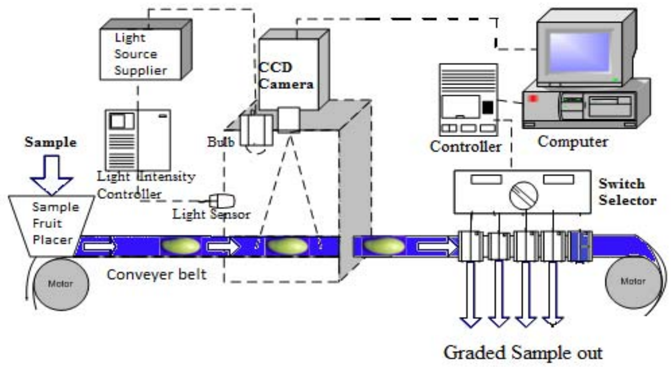

Fig.1. Proposed model of vision based automated fruit grading and sorting system.

The camera was interfaced with a computer through USB port. The proposed algorithm was implemented in Lab VIEW ® Real Time Environment for automatic sorting. Light intensity inside the closed image acquisition chamber was controlled manually and was kept at 120 lux, measured with the help of lux meter (Instek-GLS-301).

The automated fruit sorting system consists of a motor driven conveyer belt to carry the fruits serially. The fruit placer places one fruit at a time on the belt and the belt carries it to the imaging chamber where the video image of fruit is captured by the computer through CCD camera. The proposed algorithm runs into the computer automatically to classify the fruit on the basis of maturity level and then give a direction to the sorting unit to place the mango in appropriate bin.

The sorting unit consists of four solenoid valves driven by respective drive units, which are controlled by the computer. The time delay in between image capturing of a fruit and the triggering the solenoid valve is estimated by computer on the basis of conveyer belt speed.

The color of the conveyer belt was chosen blue for two reasons. First, blue does not occur naturally in mangoes. Second, blue is one of the three channels in the RGB color space, making it easier to separate the background from the image of mango.

The image capturing chamber is a wooden box and the ceiling of the chamber is quoted with reflective material to reduce the shading effect. A CCD camera is mounted in the top center of the chamber. One fluorescent lamp is mounted at the top of the chamber. The camera is mounted right side the light source for the best imaging.

The light intensity inside the imaging chamber is measured and consequently controlled by a separate light intensity controller, which keep the light intensity constant irrespective of power supply voltage and any variation of the filament characteristics and changes in ambient environment.

However, even with the lamp current being constant, the light output of the lamp still varies resulting from the lamp ageing, filament or electrode erosion, gas adsorption or desorption, and ambient temperature. These effect cause changes in the RGB values of the images. The light intensity controller corrects for the lamp output changes, maintaining a constant short and long-term output from the lamp. The light output regulating unit is made up of a light sensing head and a controller. The (silicon based) light sensor. is also mounted near to the sample fruit inside the chamber monitors part of the light source output; the controller constantly compares the recorded signal to the pre-set level and changes the power supply output to keep the measured signal at the set level i.e. 120 lux.

The still frames are extracted from the video image at the rate of 30 frames/sec. In our systems the motor speed and distance between the two consecutive mangoes were taken as input. If the motor speed and distance between two mangoes are known then we can find a frame that will be the best still image of full mango within the imaging chamber. In our system the speed of the conveyer belt was 2ft/sec, length of the imaging chamber was 1ft and the distance between two consecutive mangoes on the conveyer belt was 1ft. So 7200 samples/hour can be sorted by our system. This rate can be increased by increasing the speed of the conveyer belt and reducing the distance between two consecutive samples in the conveyer belt. The size of the still frame was 480X640 pixels.

C. Color Calibration of CCD camera

Color calibration of CCD cameras is essential for color inspection systems based upon machine vision to provide accurate and consistent color measurements. Here we have calibrated the camera using color standard.

An image matrix for four varieties of mango having different maturity levels are shown in Fig. 2.

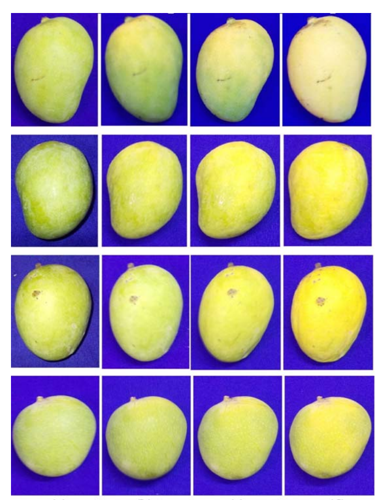

(a) (b) (c) (d)

Fig. 2. Images of four varieties mango having different maturity level. 1st row: “KU”, 2nd row: “SO”, 3rd row “LA” and 4th row “HI”. Images are taken with an interval of 2 days, shown in (a) raw (b) semimatured (c) matured (d) over-matured.

III. Pre-processing of Images

The performance of the grading system depends on the quality of the images captured from the video camera, since various measures/features calculated from the images of the mangoes will be used for grading according to maturity level. Video signal collected from camera found to be contaminated with motion artifact and noise, thus proper extraction of images from video frames and then filtering is essential. On the other hand mangoes moving through the conveyer belt, can be at any position along with the background thus in order to reduce computation, removal of background by detecting the edges of the image and alignment of the mango images in axial position is necessary. The present section discuss about all these preprocessing issues, in brief.

A. Still Frame Extraction from Video Image

At first the video streams acquired by the CCD camera are separated into sequence of images and then to remove motion related artifacts block motion compensation was employed [16]. Motion compensated four frames can be observed from Fig. 3.

(a) (b) (c) (d)

Fig.3. Extracted still frames from the video image with an interval of 5 frames, (a) frame no.10, sample entering into the imaging chamber (b) frame no.15, sample near the middle of the imaging chamber (c) frame no. 20, sample crossing the middle position of imaging chamber (d) frame no. 25, sample going out from imaging chamber.

B. Filtering of Mango Image

Though the images were taken in controlled environment under fixed illumination of light of 120 lux with the help of tungsten filament lamp, but there were some noises in the picture. To remove these noises a simple median filter found to provide reasonable good performance but it is computationally intensive. For that pseudo-median filter [17] was used in the work, as it is computationally simpler and possesses many of the properties of the median filter. This filtering process often helped to obtain smooth continuous boundary of the mango.

C. Edge Detection and Boundary Tracing

Experimentally it was observed that for all the set of the RGB mango images the G value is always greater than the B value for that reason the color of the background was kept blue with R, G and B value of close to 0, 0 and 255 respectively, as much as possible. So with the help of simple comparison the back ground was eliminated, and the image was converted to binary image (BW). Small patches containing number of pixel less than 800 were removed. This cutoff number was determined experimentally, by studying all the images of the mango.

In order to find the boundary or the contour of the mango, a graph contour tracking method based on chain-code was adopted. This algorithm found to work reasonable fast, as the boundary of the mango is not so complex.

The details of algorithm can be found in [18] here a brief description is given. The algorithm first detects every run at each row and records every single run's serial number and the corresponding start-pixel coordinates and end-pixel coordinates are stored in a table named as "ABS". Through this method, the run-length code of the image is obtained. Then, a 3×3 pixel box is adopted to detect the relationship between the objective pixel and its eight-connected surrounding pixels. All the runs are categorized into 5 classes, and then each run's serial number along with the corresponding class label was recorded in another table named as "COD". Then, the algorithm searches the ABS-table and COD-table sequentially. Based on the coordinates and class of each run recorded on the table, the starting pixel of the contour is recognized and the contour is successfully followed. And the chain code is generated while following the contour. An image of mango along with the traced boundary is shown in Fig. 4.

D. Alignment of the Mango Image

After getting the contour of the mango, search to find the longitudinal axis of the mango is obtained. Let $C(x_i, y_i), i = 1,2,....., N$ (N is the total number of points in the contour) represent the obtained contour of a mango, then two end points (x_1^l, y_1^l) and (x_2^l, y_2^l) are the points for which $l = \sqrt{(x_i^l - x_j^l) + (y_i^l - y_j^l)}$ is maximum, where $i, j = 1,2,.....N$ .After getting the coordinates of the two boundary points along the longitudinal axis the image was rotated by an angle determined by $\theta = \tan^{-1}\left[(y_2^l - y_1^l) \big/ (x_2^l - x_1^l) \right]$, this rotation will align the mango vertically but may not able to place the "apex" region at the top, it may be at the bottom position. To fix the problem another rotation of 180$^{\mathrm{o}}$ was made if the "apex" region is in bottom position. The detection of the "apex" or the "stalk" was made on the basis of geometrical properties of the varieties of the mango under test. For all the varieties of the mango the width of the apex is always higher than the stalk, this properties was utilized to place the apex region at the top of the image. The center point of the apex/stalk region is the point lies on the longitudinal axis at a distance of $0.15 \times l_{\max}$ from the two end points of the longitudinal axis. This relation was determined experimentally, and found to true for all the varieties of the mango under test.

(a) (b) (c)

Fig. 4. Filtered images of Mango, (a) raw image of a mango, (b) raw mango image along with the obtained contour, (c) binary image of the same mango after removing the small patches, also shows the different positions and their name as used in the work.

IV. EXTRACTION OF FEATURES

In order to predict the maturity level with the help of computer, some suitable measures collected from the images of the mangoes need to be investigated, which are most correlated with the maturity level. This section discuss about various features, selection of the features are mainly based on the experienced gain by the authors, while discussing this issue with the experts involves in manual grading process.

A. Average R, G and B value

This represent the average R, G and B value of the entire mango and was calculated from the following equation:

$$A_{k=R,G,B} = \frac{1}{rc}\sum_{i=1}^{r}\sum_{j=1}^{c}\left(I_k \times BW\right)$$

where, BW is the binary image acting as a mask set the region outside the contour of the mango to 0, and I_k is the captured RGB image, r and c represent the total number of rows and columns of the image.

B. Gradient of R, G and B value along the longitudinal axis

Due to the fact that the mango start ripe from the apex region, so the slope of the R, G and B varies from apex region to stalk region (shown in Fig.5), and this variation found to be different under different maturity level of the mango. The slope (I) of the R, G and B were determined by the following equation. First by taking a slice image along the longitudinal axis, the width of the sliced image is the 5% of the width of the mango at the middle position of the longitudinal axis and length in between 5% below and above of the two end points of the longitudinal axis.

$$S_{k=R,G,B} = slope\left(\sum_{i=-1}^{p} s_k(i,j)\right)$$

where p, is the width of the slice. The slope was determined by searching the best fit straight line by least mean square sense.

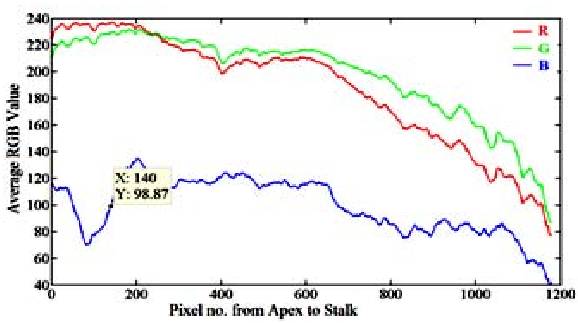

Fig. 5. Variation of R, G and B value along the longitudinal axis.

C. Average R, G and B value of the Apex, Equator and Stalk region

For collecting the average R, G and B value for these three regions, slice images along the horizontal axis were extracted from the RGB image of the mango, the width of the each slice (along the longitudinal axis) is $0.05 \times l_{\max}$ and length is in between the end points of boundary along the horizontal axis cutting the center point of each region as shown in Fig. 4 (c). The average value were calculated according to

$$As_k = \frac{1}{rc}\sum_{i=1}^{r}\sum_{j=1}^{c} Is_k$$

where Is_k, is the sliced RGB image, $k = R, G$ *and* B and $s = Apex, Equator$ *and* $Stalk$.

D. Derived Features

From these main features other derived features were calculated, these are as follows:

Differences of average R, G and B value of the entire mango i.e. $(A_R - A_G), (A_G - A_B)$ *and* $(A_R - A_B)$

Differences of corresponding average R, G and B value for the apex, equator and stalk region, i.e. $(Aapex_R - Aequator_R), (Aequator_R - Astalk_R)$ *and* $(Aapex_R - Astalk_R)$

similarly for G and B also.

The variation of the three measures i.e. average R of entire mango, average R of apex region and difference between average R to G value for the three mangoes (two from KU variety and one from HI variety) w.r.t different maturity level are shown in Fig. 6 (a), (b) and (c). From the Fig. 6 (a), (b) and (c), it can be observed that these features are correlated with the maturity level, on the other hand the nature of variation of these measures for different variety of mangoes are different. Prediction of maturity level of mango using Support Vector Machine based Regression analysis can be found in [19]. The variation of average R with respect to average G for the four different maturity levels (i.e. M1, M2, M3 and M4 of KU) is shown in Fig. 6. (d). From this figure it can be observed that these two measures are not sufficient to classify the mangoes into four different classes accurately, due to overlapping of the features, which is due to variation of color texture of different samples.

In the present work parameters of the individual classes are estimated using Gaussian Mixture Model. A brief theory of GMM is presented in next section, the details and the methods adopted in the present work for estimation of individual classes can be found in [20].

V. Gaussian Mixture Model

A Gaussian mixture density is a weighted sum of mixture component densities. The Gaussian mixture density can be described as,

$$p(\vec{x} \mid \theta) = \sum_{k=1}^{M} \omega_k p_k(\vec{x})$$

where, M is the no of mixture components and $\omega_k, k = 1,.......,M$, are the mixture weights, subject to $\omega_k > 0$ and $\sum_{k=1}^{M} \omega_k = 1$, $p_k(\vec{x})$ are the component densities and $\vec{x}$ be a d-dimensional feature vector, $\vec{x} \in \Re^d$. With $d \times 1$ mean vector μ_k and $d \times d$ covariance matrix S_k, each component density is a d-variate Gaussian function given by,

$$p_k(\vec{x}) \approx N(\mu_k, S_k) = \frac{1}{(2\pi)^{\frac{d}{2}} \mid S_k \mid^{\frac{1}{2}}} \exp\left\{-\frac{1}{2}(\vec{x} - \mu_k)^T S_k^{-1} (\vec{x} - \mu_k)\right\}$$

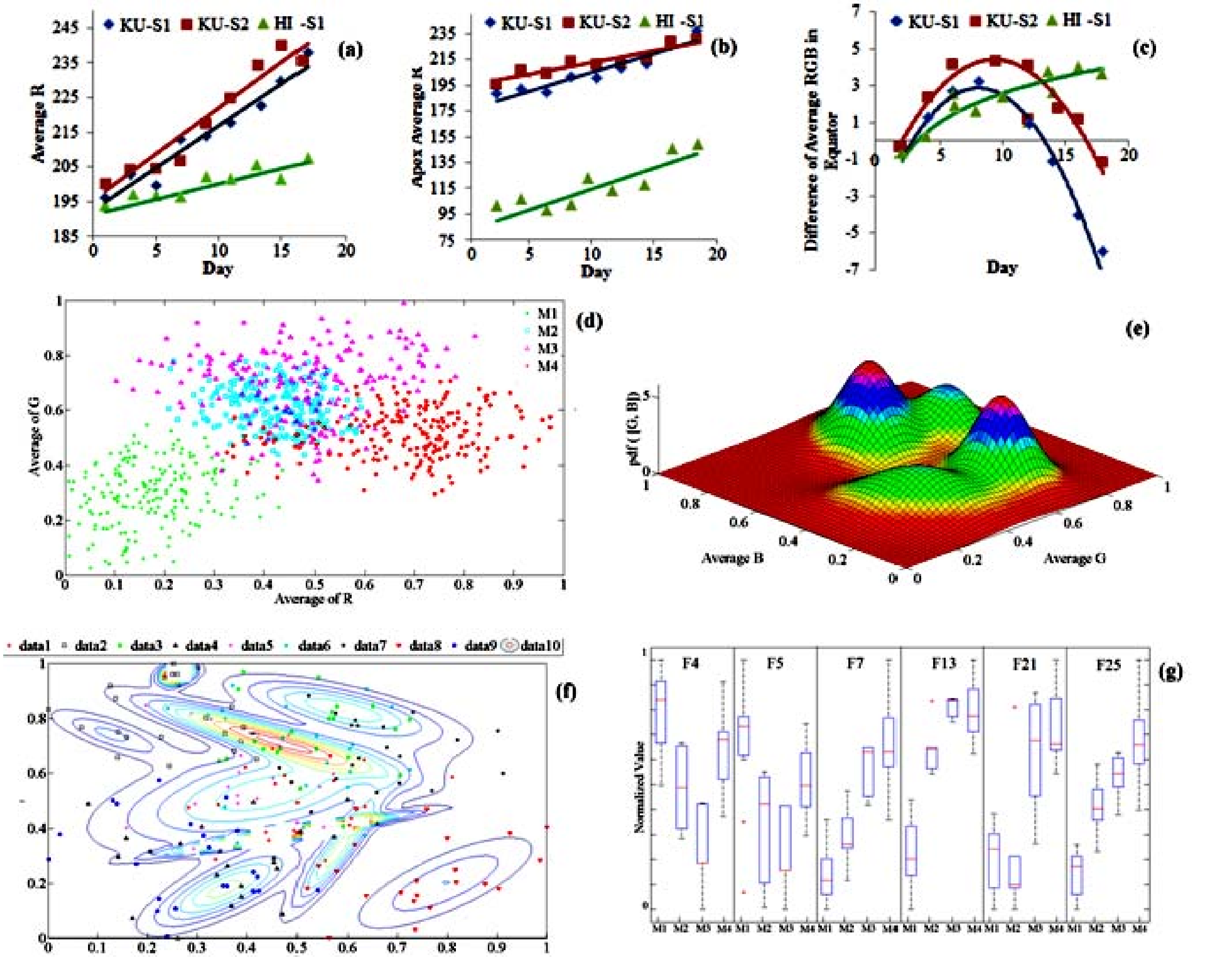

Fig. 6. Variation with maturity level (a) Average R of entire mango (b) Average R in apex region (c) Difference of average R to G. (d) Variation of average R to average G with four different maturity level(i.e. M1,M2,M3 and M4 of KU). PDF distribution with (e) average value of total G and B (f) different batches and different gardens. (g) Box-whiskers plots for most correlated features.

VI. RESULT AND DISCUSSION

The Probability Density Function (PDF) estimated using only two features i.e. Average values of total G and B values is shown in Fig. 6 (e). When the same GMM was used to find the PDF of raw mangoes came from different gardens over three batches, it was observed that there are strong correlations of the mangoes in a batch originated from a specific garden, but PDF distribution of different batches and different gardens are often found to be different. This fact can be observed from the Fig. 6. (f), where we can see that the several GMM components has been formed for the mangoes originated from different gardens and in different batches.

The summary statistics for some of the most correlated features is represented by box–whiskers plots, shown in Fig. 6. (g). The box corresponds to the inter-quartile range where top and bottom bound indicate 25th and 75th percentiles of the samples respectively, the line inside the box represents median, and the whiskers extend to the minimum and maximum values. The details of the box–whiskers plot can be found in [21].

After estimation, the evaluation of the classification performance was performed on a test data set, in which the objective was to find the class model which has the maximum a posteriori probability for a given observation sequence. The classification accuracy obtained using GMM and the average classification accuracy by the three experts for the four varieties of mango is presented in TABLE I.

VARIETY (Local Name)	M1		M2		M3		M4	
	Experts	GMM	Experts	GMM	Experts	GMM	Experts	GMM
KU	93.5	92.2	93.7	88.9	93.1	89.4	93.3	91.3
SO	92.2	91.7	92.7	88.2	92.6	89.3	91.8	90.5
LA	92.1	91.5	92.6	87.6	92.2	88.2	91.5	90.3
HI	92.1	91.4	92.2	87.4	91.7	88.5	91.3	90.3

TABLE I. PERFORMANCE ANALYSIS

From the obtained results as summarized in TABLE I, it can be observed that the classification performance for the proposed vision based automatic technique as good as the manual expert based technique. Since the accuracy is dependent on the image, which is further affected by the ambient light intensity, thus controlling the light intensity was performed. The variance in the probability density function of the features indicates the variation of color pattern of mangoes for a particular maturity level. Misclassification may occur when different maturity level mangoes having similar color pattern, but it was observed that extraction of multiple features particularly gradient based features helped to correctly identify those mangoes, as some raw mangoes having color pattern of matured mango particularly in the apex region, but those mangoes shows high gradient value of 'R' along the longitudinal axis. In some cases, the automatic technique for extraction of features failed to collect suitable features, when the surfaces of the mangoes were highly contaminated with scratches and black color patches.

VII. CONCLUSIONS

The present work is an application of machine vision based technique for automatic grading and sorting of fruits like mango according to the maturity level. Different image processing techniques were evaluated, to extract different features from the images of mango. The proposed work also aimed to find the variations of different features with maturity level of mangoes. It also shows the application of Gaussian mixture model to estimate the parameters of individual classes to predict the maturity level. This technique found to be low cost effective and moreover intelligent. The speed of sorting system is limited by the conveyer belt speed and the gap maintained in between two mangoes rather than response time of the computerized vision based system, which is on the order of ~50ms.

Test has been conducted only for the four varieties of mango, but can be extended for other fruits where there are reasonable changes in skin color texture occur with maturity. The variations of classification performances with the variation of other factors like changes in ambient light, camera resolution, and distance of the camera were not studied. The study shows that, machine vision based system performance, is closer to the manual experts, where experts judge the mangoes maturity level not only by the skin color but also with firmness and smell.

REFERENCES

[1] Jarimopas B, and Jaisin N. "An experimental Machine Vision system for sorting sweet Tamarind," Journal of Food Engineering, vol. 89(3), 2008, pp. 291 – 297.

[2] Y.Zhao, D. Wang, and D. Qian" Machine Vision based image analysis for the estimation of Pear external quality," Second International Conference on Intelligent Computation Technology and Automation, 2009, pp 629 – 632.

[3] D. J. Lee, J. K .Archibald, and Guangming Xiong. "Rapid color grading for fruit quality evaluation using direct color mapping," IEEE Trans. Autom. Sci. Eng., vol. 8(2), 2011, pp. 292– 302.

[4] Z. Varghese, C. T. Morrow, P. H. Heinemann, H. J. Sommer, Y. Tao, and R. W. Crassweller, "Automated inspection of golden delicious apples using color computer vision," American Society of Agricultural Engineers, 1991(7002), 16.

[5] B. K. Miller, and M. J. Delwiche, "A color vision system for Peach grading," Transactions of the ASAE, vol. 32(4), 1989, pp. 484 – 1490.

[6] A. Janobi, "Color line scan system for grading date fruits," ASAE Annual International Meeting, Orlando, Florida, USA, 12-16 July, 1998.

[7] Y. Tao, P. H. Heinemann, Z. Varghese, C. T. Morrow, and H. J. Sommer, "Machine vision for color inspection of potatoes and apples," Transactions of the ASAE, vol. 38(5), 1995, pp. 1555-1561.

[8] S. A. Shearer, and F. A. Payne, "Color and defect sorting of bell peppers using machine vision," Transactions of the ASAE, vol. 33(6), 1990, pp. 2045 – 2050.

[9] A. Bouganis, and M. Shanahan, "A vision-based intelligent system for packing 2-D irregular shapes," IEEE Trans. Autom. Sci. Eng., vol. 4(3), 2007, pp. 382 – 394.

[10] H. C. Garcia, and J. R. Villalobos, "Automated refinement of automated visual inspection algorithms," IEEE Trans. Autom Sci. Eng., vol. 6(3), 2009, pp. 514 – 524.

[11] H. C. Garcia, J. R. Villalobos, and G. C. Runger, "An automated feature selection method for visual inspection systems," IEEE Trans. Autom. Sci. Eng., vol. 3(4), 2006, pp. 394 – 406.

[12] S. M. Bhandarkar, X. Luo, R. F. Daniels, and E. W. Tollner, "Automated planning and optimization of lumber production using machine vision and computed tomography," IEEE Trans. Autom. Sci. Eng., vol. 5(4), 2008, pp. 677–695.

[13] N. M. Kwok, Q. P. Ha, D. Liu, and G. Fang, "Contrast enhancement and intensity preservation for gray-level images using multiobjective particle swarm optimization," IEEE Trans. Autom. Sci. Eng., vol. 6(1), 2009, pp. 145 – 155.

[14] H. Y. T. Ngan, and G. K. H. Pang, "Regularity analysis for patterned texture inspection," IEEE Trans. Autom. Sci. Eng., vol. 6(1), 2009, pp.131 – 144.

[15] Y. Cheng, and M. A. Jafari, "Vision-based online process control in manufacturing applications," IEEE Trans. Autom. Sci. Eng., vol. 5(1), 2008, pp. 140 – 153.

[16] K. Hilman, H. W. Park, and Y. Kim, "Using motion- compensated frame-rate conversion for the correction of 3 : 2 pulldown artifacts in video sequences," IEEE Trans. On Circuits and Systems for Video Technology, vol. 10(6), 2000, pp. 869 – 877.

[17] A. Rosenfeld and A.C. Kak, Digital Image Processing, New York: Academic Press, cap 11, 1982

[18] S. D. Kim, J. H. Lee, and J. K. Kim, "A new chain-coding algorithm for binary images using run-length codes [J]." CVGIP, vol. 41, 1988, pp. 114 – 128.

[19] C. S. Nandi, B. Tudu, and C. Koley "Support Vector Machine based maturity prediction," WASET, International Conference ICCESSE-2012, 2012, pp..

[20] S. Biswas, C. Koley, B. Chatterjee, and S. Chakravorty "A methodology for identification and localization of partial discharge sources using optical sensors," IEEE Trans. on dielectric and electrical insulations, vol.19(1), 2012, pp.

[21] K. Fukunaga, Introduction to Statistical Pattern Recognition, Academic Press, 1990.